Submitted, accepted and published by J. Environ. Monit., 2012, 14, 1211-1220

Apportionment of the airborne PM10 in Spain. Episodes of potential negative impact for human health

M.S. Callén*, J.M. López, A.M. Mastral

Department of Energy and Environment, Instituto de Carboquímica (ICB-CSIC), Zaragoza, 50018, Spain

*Corresponding author: E-mail: *marisol@icb.csic.es*, Tel +34 976 733977, Fax: +34 976 733318

Abstract

The particulate matter with an aerodynamic diameter less or equal than 10 and 2.5 microns respectively (PM10 and PM2.5) constitutes one of the main air pollutants, which is currently regulated in Europe through Directive 2008/50/EC due to its proven harmful effects on human health. In this paper, the airborne PM10 samples collected in Zaragoza city during 2001-2009 were apportioned by statistical tools based on principal component analysis with absolute principal component scores (PCA-APCS). PM10 samples were characterized regarding their concentrations on polycyclic aromatic hydrocarbons (PAH) and water soluble ions. PAH were analyzed by gas chromatography-mass spectrometry-mass spectrometry detection (GC-MS-MS) and ions were analyzed by ion chromatography. A total of five factors were identified by PCA-APCS corresponding to different anthropogenic and natural sources. This work was focused on analyzing in more detail those samples involving higher negative impact on human health, in particular, PM10 samples exceeding the daily PM10 limit value of 50 μg m^{-3} according to Directive 2008/50/EC and samples with concentrations of benzo(a)pyrene (BaP) higher than the upper assessment threshold (BaP>0.6 ng m^{-3}) established by the Directive 2004/107/EC. Most of the exceedances of the daily PM10 limit value were associated with direct and indirect North-African long-range transport.

During these exceedances, it was observed that anthropogenic pollution sources slightly decreased with regard to the natural sources. This indicated that episodes of high PM10 could have a natural origin associated with long-range transport from African continent. On the contrary, those exceedances with regional contribution and samples with BaP concentrations higher than 0.6 ng m^{-3} showed an important contribution of anthropogenic pollution sources increasing their negative impact on human health.

Keywords: PM10; PAH; ions; PCA-APCS; air pollution.

1. Introduction

Air quality is a main concern issue due to population is continuously exposed to air pollutants affecting the whole planet. The particulate matter is one of the main pollutants of varied nature which is regulated through different European Directives [1,2] and with proven harmful effects on human health. These harmful effects are depending on, not only the particle size but also the nature of the particulate matter. A special family of organic pollutants that can be composing the particulate matter are polycyclic aromatic hydrocarbons (PAH) with carcinogenic and/or mutagenic character[3] and also regulated through European Directives [4]. This negative impact on human health and the fact that PAH are trans-boundary pollutants requires improving knowledge regarding the main sources producing these pollutants. Information on the sources of environmental pollution is clearly vital in integrated impact assessment, for modelling environmental pollution, to estimate changes in technology or policies and to identify where preventative actions can be best taken. Source attribution is based on the principle that, measured exposures to a pollutant or other hazard are the result of a process of release, transport and transformation. One of the statistical tools that provides information to identify air pollution sources is the principal component analysis (PCA), which has been applied to airborne particulate matter [5,6] as well as PAH[7]. A specific application is the PCA with absolute principal component scores (PCA-APCS) established by Thurston and Spengler, 1985[8] and successfully applied for source apportionment of pollutants in the atmosphere [9-12].

In this work, the PCA-APCS receptor model was used to apportion the airborne PM10 of Zaragoza during three different sampling periods (2001-2009) carried out in Zaragoza. The aim was to contribute to improve knowledge on PM10 source apportionment in order to fulfil air quality policies. Once characterized the concentrations of PAH and ions contained in the PM10, special attention was paid out to those samples exceeding the daily limit value of PM10 and samples with concentrations higher than the upper assessment threshold of BaP due to their negative potential impact on human health. A comparison of the contribution of anthropogenic and/or natural sources was carried out.

2. Experimental

2.1 Sampling description

The study was performed in Rio Ebro campus (length= 41.68, latitude= -0.89), Zaragoza city, located in the North-East of Spain, in an urban area close to a highway (AP-2, daily average traffic intensity in 2009 =13025 vehicles), several industrial parks related to medium and small enterprises located along the main roads, three paper fabrics and three waste water treatment plants (Fig. 1). In the Teruel province, there are three power stations using coal as main fuel, one of them with a power of 1050 MW is located in the SE direction from the sampling point. The sampling site is close to agricultural pastures located at the Ebro River and several construction activities were carried out in the vicinity of the sampling site during 2007-2008 for the International Expo celebrated in 2008. There are also different gypsum mountains along the Z-40 road from the Madrid to the Castellón road (SW direction). The population of the city of Zaragoza was 701090 inhabitants in the first of September of 2010. Zaragoza shows a Continental Mediterranean climate with drier summers and winters and wetter springs and autumns similar to a semi-arid climate as it is localized in a wide basin entirely surrounded by mountains. The yearly average precipitation is 310 mm with abundant sunny days whereas the rainfall centres in spring and there is drought in summer. The temperatures are high in summer reaching up to 40 °C whereas in winter the temperatures are low (usually 0 to 10 °C) either because of the fog (about 20 days from November to January) or a cold

and dry wind blowing from the NW, the Cierzo on clear days. Frost is common and there is sporadic snowfall.

2.2. PM10 sampling

A GUV-15H Graseby Andersen high-volume sampler with volumetric flow controlled system provided with a PM10 cut off inlet at 10 μm and located 3.5 m from the ground was used to collect the particulate phase in a PTFE-coated, glass-fibre filter (0.6 μm pore size; 20.5 cm × 25.5 cm, Pall GelmanSciences). Samples were captured during 24 hours every two weeks from November 15th, 2001 to July 26th, 2002, every week from April 7th, 2003 to July 5th, 2004 and finally, during consecutive days from May 23th to June 6th 2008 and from January 13th to 27th 2009 collecting a total of 112 samples with average air volumes around 1600 m^3.

Before the sampling, filters were Soxhlet extracted for 24 h with dichloromethane (DCM) and kept in desiccators. Once conditioned, filters were weighted before and after the sampling using a micro-analytical balance (precision of 0.01 mg) to determine the particle mass. After sampling, filters were wrapped in aluminium foil previously rinsed with hexane and stored in a freezer at -20 ºC until analysis[13-15].

2.3 Ion analysis

One-eight of the filter was cut in small pieces and extracted by ultrasonic bath for 30 minutes in 15 mL of Milli-Q water. The obtained solution was filtered through cellulose acetate membrane filters (0.2 μm pore size and 30 mm filter diameter) until a final volume of 15 mL. Analyses were carried out by a Dionex ICS2000 ion chromatography system with Chromeleon version 6.60SP2 software[13]. The anion and cation methods used the AS17 analytical column (2 mm × 250 mm) and the CS17 analytical column (3 mm × 250 mm), respectively. In both cases, the detector was a conductivity cell working at 35 ºC. An eluent suppressor working at 19 mA (anions) and 62 mA (cations) was placed before the detector in order to prevent saturation by the background signal[12].

A total of four anions (Cl^-, NO_2^-+NO_3^-, SO_4^{2-}) and three cations (Na^+, Mg^{2+}, Ca^{2+}) were detected and quantified by using different concentrations of standards mixture from respective ions. The sulphate concentration of marine origin, mSO_4^{2-} was determined indirectly by considering the Na^+ soluble concentration according to the ratio: mSO_4^{2-}/Na^+= 0.25 in weight [16]. The non-sea-salt-sulphate, $nssSO_4^{2-}$, generally of anthropogenic origin, was obtained by subtracting the total SO_4^{2-} concentration to this value.

The detection and quantification limits were determined according to three and ten times the blank standard deviation (the lowest detection limit for SO_4^{2-}: 0.074 mg L^{-1}, the highest detection limit for Na^+: 0.530 mg L^{-1}). Analyses of the standard reference material SRM 1944 provided by the National Institute of Standards and Technology (NIST) were carried out in order to check the analytical accuracy and precision of ions. Measured values were satisfactorily comparable to certified values with deviations lower than 16% for ions.

2.4 PAH analysis

One-fourth of the filter was extracted by Soxhlet during 18 hours with DCM after the addition of deuterated-PAH surrogate standards containing the following PAH: anthracene-d_{10} (An-d_{10}), benzo[a]pyrene-d_{12} (BaP-d_{12}) and benzo[ghi]perylene-d_{12} (BghiP-d_{12}). Extracts were concentrated on a rotary evaporator followed by a stream of nitrogen gas. Samples were cleaned-up through a silica gel column and eluted with DCM. Then the eluted sample was evaporated using a gentle nitrogen gas stream and the extract reconstituted with an internal standard solution (p-terphenyl) in hexane. Samples were analysed by gas chromatography-mass spectrometry-mass spectrometry detection (GC-MS-MS)[15]. PAH quantification was performed using the internal standard method relative to the closest eluting PAH surrogate. The p-terphenyl was added to the sample previous to the analysis by GC-MS-MS in order to calculate the deuterated PAH's recovery.

All analyses were carried out on a Varian GC 3800 gas chromatograph coupled to a Saturn 2200 mass spectrometer detector. A low bleeding Factor Four capillary column (VF-5 ms: length: 30 m, ID: 0.25 mm; film thickness: 0.25 μm) was used and the temperature time program was the

following: 60 °C isotherm for 1 min, 10°/min till 300 °C and isotherm for 20 min. The injector was kept at constant temperature of 280 °C. High purity helium was used as carrier gas at a flow rate of 1 ml/min and transfer line was heated at 280 °C. In all cases, 1 μl of sample was injected in splitless mode. The ion trap mass spectrometer was operated in electron ionization (EI) mode (70 eV), the filament emission current was 80-90 μA, the scan time was 0.5 s/scan and the scanned mass range: 40-650 m/z. The transfer line and the ion trap were set to 280 and 200°C, respectively. The MS-MS process was conducted by collision induced dissociation (CID) in the resonant excitation mode. All the specific conditions for the PAH quantification by GC-MS-MS as well as the different PAH, abbreviations, the number of benzene and total rings and their vapour pressures[17] are shown in Table 1.

Seven-point multi-point calibration curves for all PAH, ranging from 20 ng mL^{-1} to 1000 μg mL^{-1}, were obtained ($r > 0.98$). The precision of the GC-MS method was checked in terms of relative standard deviation (RSD) of the internal standard response factors. RSD values relative to the closest eluting PAH surrogate ranged from 4% to 9%. The method quantification limits varied between 110 pg m^{-3} (Phe) and 6 pg m^{-3} (BaA and Chry). Analyses of the standard reference materials SRM 1649a provided by NIST were carried out in order to check the analytical accuracy and precision of PAH. Measured values were satisfactorily comparable to certified values with deviations lower than 23%.

2.5 PCA model

Principal component analysis (PCA) was applied to all samples by using software package SPSS version 15.0. Firstly, all variables were typified and transformed into a dimensionless standardized form. In order to choose the variables providing a more feasible solution, communalities were checked. Results from all PCA analyses were evaluated only for factors with eigenvalues higher than unity by adopting the Kaiser criterion. Chemical variables were considered to identify source categories only when factor loadings were >0.7 (absolute value). Afterwards, absolute principal component scores (APCS) method was used to quantify the contributions of all sources to each

measured pollutant by using the methodology established by Thurston and Spengler, 1985 [8]. Subsequent multiple linear regression (MLR) of sample mass concentration on these APCS derived estimated mass concentration of each source.

2.6. Backward air mass trajectories

The long-range atmospheric transport was deduced by determining isentropic backward trajectory analysis using the Hybrid Single-Particle Lagrangian Integrated Trajectory model (HYSPLIT)[18] with EDAS meteorological input. The backward air trajectories arriving at the sampling site during the five days previous to sampling were performed at 500, 1500 and 2500 m, respectively in order to check the air masses origin for each day of the campaign. Trajectories were classified according to Pérez *et al.* (2008)[19] where the origin sector of air masses are: (ANW) North-West Atlantic, (AN) North Atlantic, (AW) West Atlantic, (REG) regional recirculation in the Iberian Peninsula, (ASW) South-West Atlantic, (EUR) European scenario and (NAF) North-African episodes.

3. Results and discussion

3.1. PM10

A summary of the average PM10 concentrations collected in Zaragoza as well as all the analyzed species is reported in Table 2. Regarding the PM10 concentrations, it was observed that the average concentration was 32.9 $\pm$15.2 μg m^{-3}, lower than the annual (40 μg m^{-3}) PM10 limit value established by the European Directive 2008/50/EC[4]. However, episodes exceeding the daily PM10 limit value (50 μg m^{-3}) were obtained and they will be commented in Section 3.5.

These PM10 concentrations were similar to the ones reported by other authors in an urban background site in Lecce, Italy[20] (26.3 μg Nm^{-3}), in a city sampling site in Viena, Austria[21] strongly influenced by traffic emissions (32.5μg m^{-3}) and in Pamplona and Alsasua, Spain[22] (28.8 and 27.7 μg m^{-3}, respectively), two cities representing urban background. Querol *et al.* (2004)[23] compiled PM10 data in different countries in Europe. The urban background sites in Germany (28-38 μg m^{-3}), in Spain (31-42 μg m^{-3}) and the roadside stations in United Kingdom (35 μg m^{-3}) and the

Netherlands (30 μg m^{-3}) showed results comparable to this study, corroborating that the PM10 concentrations reported in this work were within the typical range reported for urban samples [24,25]. Nevertheless, PM10 concentrations higher than the ones reported in this study were obtained in an urban station located in Elche, Spain[26] (48.4 μg m^{-3}) and in an industrial Northern city, Torino, Italy[27] with average PM10 concentrations of 46.1±28.8 μg/m^3 during 2003-2004. Massaud *et al.* (2011)[28] also reported high PM10 concentrations in Beirut (54.7 μg m^{-3}, 60.7 μg m^{-3} and 74.7 μg m^{-3}, respectively) and also higher PM10 concentrations were reported in Fushun, China[29] in different industrial sites varying from 62.0 to 226.3 μg m^{-3}.

3.2. Ionic composition of PM10

The ionic species followed the order: SO_4^{2-}>NO_3^-> Ca^{2+}>Cl^->Na^+>K^+ with the most abundant anions SO_4^{2-} and NO_3^-. This predominance of SO_4^{2-} versus NO_3^- was also reflected during the warm season (summer and spring) corroborating the enhanced SO_4^{2-} concentration due to the increased photochemical activity reported by different authors [30] during the warm season. On the contrary, the winter period with low temperature and high relative humidity favoured the formation of NO_3^- [31] versus SO_4^{2-}.

The most important sources of NO_3^- and SO_4^{2-} in the atmosphere are the secondary aerosols produced by oxidation of their gaseous precursors, NO_2 and SO_2, respectively, emitted from various anthropogenic activities. In Zaragoza, SO_4^{2-} may be released from different local pollution sources like industry, coal combustion as well as diesel combustion and oil-fired power plants, which contain higher sulphate concentrations than most of the coal-fired power plants. Other main source is due to mineral aerosols. The average percentage of nmSO_4^{2-} versus SO_4^{2-} was 95.6% indicating that its main source had anthropogenic origin. In Zaragoza, SO_4^{2-} represented 11% in weight of the PM10 and it was correlated at 99% level with K^+ and Ca^{2+} indicating that the main form of non-marine sulphate was K_2SO_4 and $CaSO_4$.

The main sources of NO_3^- are coal and biomass combustion, industry and traffic emissions, all of them local sources that play a major role near the Zaragoza monitoring site. NO_3^- represented the

9% in weight of the PM10 and it showed a positive and significant correlation at 99% level with SO_4^{2-}, Cl^-, K^+ and at 95% level with Ca^{2+} indicating that these ions could have a similar emission source associated with fossil fuel combustion including vehicular emissions. Cl^- represented a 2% in weight of the PM10. The Cl^- to Na^+ ratio in this work was 1.11, lower than the value of 1.8 in sea water indicating significant chloride depletion mainly in summer. Higher ratios in winter corroborated not only the marine origin but also the contribution of other anthropogenic sources like different paper fabrics located around the city.

With regard to the cations, Ca^{2+} was the most abundant one representing 3.6% in weight of the PM10 and it could reflect the impact of construction activities, soil resuspension and unpaved roads [32]. K^+ represented 0.9% in weight of the PM10. Its main origin sources, in addition to the marine aerosol and soil resuspension, could be anthropogenic sources like forest fires, agricultural or biomass burning. K^+ has been used as a biomass burning tracer in source apportionment [33]. The presence of waste incineration plants and paper fabrics located in the surroundings of the city could justify this contribution. In fact, its positive and significant correlation with NO_3^-, $nmSO_4^{2-}$, Cl^-, Ca^{2+} and Na^+ also corroborated its possible anthropogenic origin.

3.3. Particulate-phase PAH

The individual and the total average PAH concentrations bound to the PM10 with the corresponding standard deviations for the different years of sampling are summarized in Table 2. It is worth pointing out that only PAH in the particulate phase were collected in these campaigns so that low concentrations of the most volatile PAH were expected as shown in Table 2. Gas/particle partitioning of these compounds is affected by the physicochemical characteristics of the aerosol (chemical composition, particle size, surface area) and the ambient conditions (temperature, pressure) and the most volatile PAH are found predominantly in the vapour phase[34] whereas 90% of 5-6 ring PAH are absorbed on particles. However, our main aim was to collect the high molecular weight PAH due to these are more harmful for human health.

The most abundant PAH were IcdP+DahA, BghiP, Cor, BbjkF and Chry. Together, these compounds accounted for around 67% of the total PAH. BghiP, BbF and IcdP represented the highest proportions of the total PAH concentration in La Plata, Argentina and Leipzig, Germany[35]. In addition to BaP and DahA, BghiP in particular identified traffic as the main source of urban PAH emissions. BbkF and Chry were also the most abundant PAH in the PM10 in an urban site in Elche, Spain[36] indicating the dominant source of vehicle emissions.

One of the most interesting PAH used as indicator of carcinogenic risk is BaP. By comparing published results on BaP around the world, it is possible to observe that higher BaP concentrations were reported in an industrial region in Hong Kong, China [37] (0.94 ng m^{-3}), in Mexico city, Mexico[38] during the dry season (0.786 ng m^{-3}) although very similar concentrations were obtained during the rainy season (0.322 ng m^{-3}). Similar BaP concentrations to the ones reported in this work were also observed in La Plata, Argentina[35] (0.381 ng m^{-3}), in Las Palmas de Gran Canaria, Spain[39] (0.34 ng m^{-3}) and in Sao Paulo, Brazil [40](0.28 ng m^{-3}) close to a highway. Lower BaP concentrations were reported by Varea *et al.* [36](2011) in an urban site in Elche, Spain (0.177 ng m^{-3}) and in Leipzig, Germany[35] (0.148 ng m^{-3}) in 1999-2002. Nevertheless, the comparisons must be done with caution due to the influence not only of the sampling site but also, the year of sampling, the meteorological conditions and the different sampling, clean-up and analysis procedures that may influence on the PAH partitioning between the gas and particulate phases.

3.4. Source apportionment of the airborne PM10 by PCA-APCS

Once characterized the organic and inorganic component of the PM10, PCA with Varimax rotation was applied to all samples in order to know the emission sources associated to these pollutants. Statistical criteria for the different chemical families allowed selecting the following significant variables: Phe, An, 2,4 MePhe, Flt, Py, BaA, Chry, BbjkF, IcdP+DahA, BghiP, Cor, Cl^-,NO_3^-, $nmSO_4^{2-}$, Na^+, Ca^{2+} and K^+ always verifying that n>30+(V+3)/2 where n= number of samples and V= number of variables [41]. PCA with Varimax rotation distinguished a total of five factors

explaining 85% of the variance and they were associated with different anthropogenic and natural sources (Table 3).

The first factor explained 42.9% of the variance and it was related to BbjkF, BeP, BaP, BaA and Chry. BeP and BaP are markers for light oil burning [42], which is used for domestic heating and many industrial processes. Nevertheless, BbF, BeP and BaP are also found in the ambient air at the traffic source [43] and BaA and Chry, tracers of natural gas, were also included in this factor reflecting the major use of this fuel for domestic heating in Zaragoza. Therefore this factor could be associated with industrial emissions, domestic heating and vehicular emissions.

The second factor explaining 17.6% of the variance was associated with An, Phe, MePhe, Flt and Py. Flt, Py and Phe are components of fossil fuels and a portion of them is associated with their combustion [44] mainly coal combustion so this factor was considered like coal combustion. The third factor explaining 11.7% of the variance was related to Cor, BghiP and IcdP+DahA. These three PAH are typical markers of traffic emissions[45] and IcdP was associated with diesel emissions[46]. High concentrations of Cor have also been found in areas using diesel as main fuel and with high density of traffic[47]. The presence of a highway close to the sampling point could explain this factor named as heavy-duty vehicle. The fourth factor explaining 7.5% of the variance was related to $nmSO_4^{2-}$, Ca^{2+}. In addition to the anthropogenic origin of non-marine sulphate due to the oxidation of fossil fuel combustion products, this can also have natural origin explained by the presence of gypsum deposits and quarries of limestone, which are also used as construction materials[48]. This factor was labelled as soil resuspension and abrasions from construction materials such as cement. The fifth factor explained 5.4% of the variance and it was associated with Cl^- and Na^+. This component was associated with marine components due to Zaragoza is almost equidistant from both the Cantábrico and Mediterranean Seas.

The absolute principal component scores (APCS) method and the subsequent multiple linear regression (MLR) applied to these APCS estimated mass concentrations of each source. A good correlation between the experimental and the modelled PM10 was found (R^2=0.77) (Figure. S1,

Supplementary information) with a slope of 0.99, suggesting the applicability of this receptor model to estimate PM10 source contributions. According to this receptor model, the main sources of PM10 were attributed to 66% soil resuspension, 8% industrial+traffic emissions, 3% coal combustion, 3% marine component and 1% heavy-duty vehicles, un-explaining 19% of the PM10 (6.32 $\mu g/m^3$) (Fig. S2, Supplementary information). The temporal evolution of each factor is shown in Fig. 2. Only the coal combustion factor showed no seasonal behaviour indicating that its behaviour was similar along the year. This could be influenced by the presence of power stations localized in Teruel as well as different industrial parks using mainly coal as fuel. The other three factors: industrial+traffic emissions, heavy-duty vehicles and marine component showed maximum average contributions during the cold season (winter, autumn) whereas the soil resuspension factor showed high concentrations during the warm season. This trend of the soil resuspension factor is typical of the Mediterranean countries and it is favoured by meteorological conditions such as: high temperature, high isolation ratio, high atmospheric pressure, low precipitations and the convective meteorology, that favours the soil resuspension. Moreover, there is an important contribution of calcium-rich aerosol in these countries due to the high frequency of Saharan air mass intrusions and the long range transport of airborne material. In the industrial+traffic emission factor, in addition to the light oil and natural gas used in industrial parks, the natural gas mainly used for domestic heating in Zaragoza would also contribute to this factor showing maximum contributions during the cold season. The marine component also showed higher contributions during the cold season due to air masses transported from the West Atlantic Ocean and the Mediterranean Sea. Seasonally, the Atlantic sectors (AN, ANW and AW) are more frequent during the cold season whereas the trajectories from the South (ASW, AFR) are the predominant ones during the warm season. The trajectories with AN origin are caused by the circulation around the Azores anticyclone affecting frequently to the Iberian Peninsula. The AW and ASW trajectories are not so often due to the meteorological factors originating this phenomenon are not so common. The first one (AW) is typically associated with the circulation originated by low pressures approaching to the occidental

coast of Europe from the Atlantic. The second one (ASW) is related to the cyclonic circulation around low pressure systems located to the Western Portugal or over the Iberian Peninsula. The particulate matter concentrations obtained during the Atlantic transport (AN, ANW, AW) showed a major marine origin with low PM10 concentrations due to phenomena associated with rainfall[22].

The chemical profile of each element was also obtained by following the method developed by Thurston and Spengler (1985)[8] with subsequent MLR. The dependent variable was the concentration of the different chemical species analyzed and the independent variables were the daily contributions of each source. Table 4 shows the contribution of each variable to the different factors obtained by the PCA-APCS receptor model. It is shown that PAH contributed majority to the anthropogenic sources whereas ions were the major components of the partial natural sources.

3.5. Exceedances of the PM10 limit value

Because of proven high levels of particulate matter are related to harmful effects on human health including asthma, respiratory problems and even cancer, special attention was paid to those PM10 samples exceeding the daily limit value of 50 μg m^{-3} established by the European Directive [1]. Fourteen percent of the PM10 samples exceeded this daily limit value (average PM10 concentration of these episodes= 60.13 μg m^{-3}) and 56% of the exceedances were produced during the warm season including spring and summer seasons whereas the other 44% exceedances were produced during the months of December and January.

A study of the backward air trajectories was performed for those samples exceeding the daily PM10 limit value, classifying these episodes with regard to the air masses origin according to Pérez *et al.* (2008)[19]. Most of these exceedances (69%) were influenced by long-range transport from the North African continent including the indirect African intrusions through the Mediterranean Sea with regional recirculation (NAF+REG). Only one episode (6% of the samples) was considered as European (EUR) with possible PM10 contribution due to long-range transport from some European countries and 25% of the exceedances were classified as regional episodes (REG) when the backward air trajectories stayed at the Iberian Peninsula showing no influence of African dust.

Fig. 3 shows a comparison of the source contributions obtained by the PCA-APCS receptor model for the total samples, the PM10 exceedances and the PM10 exceedances classified according to the HYSPLIT model during the 2001-2009 sampling. It was observed that partial natural sources related to soil resuspension were the major factor contributing to the PM10 independently of the scenario. However, concerning the exceedances of PM10, the NAF+REG episodes increased the contribution of the soil resuspension factor whereas the regional episodes with no North-African contribution (REG) increased considerably anthropogenic sources like industrial+traffic emissions by decreasing the soil resuspension factor. By studying the meteorological variables, it was observed that the temperature was the only variable statistically significant different between the two types of episodes. In the case of the NAF+REG episodes, the average temperature was 21ºC whereas in the case of REG episodes, the average temperature was 9ºC, favouring the high temperature the North-African intrusions. With regard to the only European episode and comparing to the average PM10 samples and PM10 exceedances, its soil resuspension contribution decreased by increasing the industrial+traffic emission factor, attributing this fact not only to local emission sources but also to long-range transport from European countries. This helped to understand that exceedances of the daily PM10 limit value could have different impact on human health depending on the air masses origin. In general, direct and/or indirect North-African episodes had less contribution of anthropogenic sources than regional episodes with no African contribution indicating that these last episodes of high PM10 concentrations could be more dangerous for human health.

A study of these PM10 exceedances was also performed as a function of the season by classifying high PM10 concentrations in two groups: cold season (autumn and winter) and warm season (spring and summer) (Fig. 4). It was observed that for the exceedances of the PM10 during the cold season, the heavy-duty vehicles and the industrial+traffic emission factors constituted more than the 20% of the PM10 and the resuspension factor involved the 78% of the PM10 (Fig. 4a). The exceedances produced during the warm season decreased to 8% the contribution of anthropogenic pollution

sources by increasing the soil resuspension factor to 90%. This indicated the different character of PM10 exceedances depending on the meteorological conditions, with a higher negative impact on human health of those exceedances produced during the cold season due to a higher contribution of anthropogenic sources. When these exceedances were also studied as a function of the backward air mass trajectories (Fig. 4b), it was observed that NAF+REG episodes during the cold season showed an increase in anthropogenic sources related to industrial+traffic emissions when compared to NAF+REG episodes produced during the warm season. This was also corroborated for the REG episodes being potentially more harmful for human health the PM10 exceedances produced during the cold season than the ones originated during the warm season. The long-range transport from European countries only was reflected during the cold season showing as well a decrease of natural sources related to soil resuspension and an increase of the industrial+traffic emissions factor when compared to the average PM10 exceedances. These results proved the relevance of characterising PM10 exceedances in Mediterranean countries like Spain due to their different impact on human health.

3.6. Episodes of high BaP concentrations

The carcinogenic and mutagenic properties of PAH and the fact that BaP is used as a marker for the carcinogenic risk of PAH in ambient air through the European Directive 2004/107/EC[4], made to study in more detail those episodes with high BaP concentrations. Rather than considering the target value of BaP proposed by the mentioned Directive (BaP= 1.0 ng m^{-3} for the total content in the PM10 fraction averaged over a calendar year), episodes exceeding the upper assessment threshold of BaP (0.6 ng m^{-3}) were analyzed. A total of eighteen dates exceeded this threshold, 94.4% were produced during the cold season (winter and autumn) with 67% during the winter. This fact corroborated the higher negative impact of anthropogenic sources during this period due to typical winter meteorological conditions (low temperature, low solar irradiation) as well as domestic heating contribution.

Fig. 5 shows the sources contribution of the five factors found by PCA-APCS for those episodes exceeding the upper assessment threshold of BaP as a function of the year of sampling. It is observed that comparing to the average total samples, the episodes exceeding the upper assessment threshold of BaP showed a decrease in the soil resuspension factor whereas the industrial+traffic and coal combustion factors were the predominant anthropogenic pollution sources. This corroborated that PAH had a main anthropogenic origin and mostly this anthropogenic contribution was produced during the cold season involving a higher risk for human health when compared to the average total samples.

4. Conclusions

The PCA-APCS receptor model allowed the identification and quantification of five sources in the PM10 of Zaragoza: anthropogenic sources related to industrial+traffic emissions, coal combustion and heavy-duty vehicles and partial natural sources associated with soil resuspension and marine component.

Samples representing higher risk for human health, it means samples exceeding the daily PM10 limit value according to Directive 2008/50/EC and concentrations of BaP higher than the upper assessment threshold established by the Directive 2004/107/EC, had different contributions in natural and anthropogenic sources depending on the nature of the air masses origin. Those PM10 exceedances with North African intrusion or indirect intrusion through the Mediterranean Sea showed an increase in the soil resuspension factor whereas those with regional recirculation increased the anthropogenic contribution. Regarding the season, it was also observed that PM10 exceedances during the cold season presented a higher negative impact on human health than those produced during the warm season with mainly contribution of soil resuspension factor. Samples exceeding the upper assessment threshold of BaP also showed an important contribution of anthropogenic pollution sources like industrial+traffic and coal combustion factors and a decrease in natural sources. This reflected the different impact that the nature of the samples could have on

human health, with a more negative impact on human health for those samples with higher contribution of anthropogenic sources.

Acknowledgements

Authors would like to thank Aula Dei-CSIC (R. Gracia) for providing the meteorological data as well as the Ministry of Science and Innovation (Spain)(MICIIN) and the E-Plan for partial financial support through the project CGL2009-14113-C02-01. J.M. López would also like to thank the MICYT for his Ramón y Cajal contract. We also acknowledge the NOAA Air Data Resources Laboratory and the Australia's Bureau of Meteorology for the HYSPLIT model.

References

1. Directive 2008/50/EC of the European Parliament and of the Council of 21 May 2008 on ambient air quality and cleaner air for Europe, 2008.
2. Directive 1999/30/EC of 22 April 1999 relating to limit values for sulphur dioxide, nitrogen dioxide and oxides of nitrogen, particulate matter and lead in ambient air, 1999.
3. A. Luch, *The Carcinogenic Effects of Polycyclic Aromatic Hydrocarbons*. Imperial College Press, ISBN 1-86094-417-5, London, 2005.
4. Directive 2004/107/EC of the European Parliament and of the Council of 15 December 2004 relating to arsenic, cadmium, mercury, nickel and polycyclic aromatic hydrocarbons in ambient air, 2004.
5. A. Arruti, I. Fernández-Olmo, A. Irabien, *J. Environ. Monit.,* 2010, **12,** 1451-1458.
6. L. Bencs, K. Ravindra, J. de Hoog, E. O. Rasoazanany, F. Deutsch, N. Bleux, P. Berghmans, E. Roekens, A. Krata, R.Van Grieken, *J. Environ. Monit.*, 2008, **10**, 1148-1157.
7. B. Han, X. Ding, Z. Bai, S. Kong, G. Guo, *J. Environ. Monit.,* 2011, **13**, 2597-2604.
8. G.D. Thurston and J.D. Spengler, *Atmos. Environ.,* 1985, **19(1)**, 9-25.
9. P. Bruno, M. Caselli, G. de Gennaro, P. Ielpo, B.E. Daresta, P.R. Dambruoso, V. Paolillo, C.M. Placentino, L. Trizio, *Microchem. J.,* 2008, **88**, 121-129.
10. M.L.D.P. Godoy, J.M. Godoy, L.A. Roldao, D.S. Soluri and R.A. Donagemma, *Atmos. Environ.,* 2009, **43**, 2366-2374.
11. H. Guo, A.J. Ding, K.L. So, G. Ayoko, Y.S. Li and W.T. Hung, *Atmos. Environ.,* 2009, **43**, 1159-1169.
12. M.S. Callén, M.T. de la Cruz, J.M. López, M.V. Navarro and A.M. Mastral, *Chemosphere,* 2009, **76**, 1120-1129.
13. M.S. Callén, M.T. de la Cruz, J.M. López, R. Murillo, M.V. Navarro and A.M. Mastral, *Water Air Soil Poll.,* 2008, **190**, 271-285.
14. J.M. López, M.S. Callén, R. Murillo, T. Garcia, M.V. Navarro, M.T. de la Cruz, A.M. Mastral, *Environ. Res.*, 2005, **99**, 58-67.
15. M.S. Callén, M.T. de la Cruz, J.M. López, R. Murillo, M.V. Navarro and A.M. Mastral, *Chemosphere*, 2008, **73**, 1357-1365.
16. R.A. Duce, R. Arimoto, B.J. Ray, C.K. Unni and P.J. Harder, *J. Geophys. Res.,* 1983, **88**, 5321-5342.
17. ToxProbe, Benzo[a]pyrene and other polycyclic aromatic hydrocarbons, Research Report Prepared by ToxProbe Inc. for Toronto Public Health (Canada), 2002, pp. B78-B95, http://www.toronto.ca/health/pdf/cr_appendix_b_pah.pdf.

18. R.R. Draxler, HYSPLIT4 user's guide. NOAA Tech. Memo. ERL ARL-230, NOAA Air Resources Laboratory, Silver Spring, MD, 1999.
19. Pérez, J. Pey, S. Castillo, M. Viana, A. Alastuey and X. Querol, *Sci. Total Environ.,* 2008, **407**, 527-540.
20. D. Contini, A. Genga, D. Cesari, M. Siciliano, A. Donateo, M.C. Bove, M.R. Guascito, *Atmos. Res.* 2010, **95**, 40–54.
21. A. Limbeck, M. Handler, C. Puls, J. Zbiral, H. Bauer, H. Puxbaum, *Atmos. Environ.,* 2009, **43**, 530–538
22. J. Zabalza, D. Ogulei, D. Elustondo, J. M. Santamaría, A. Alastuey, X. Querol, P. K. Hopke, *Environ Monit Assess*., 2007, **134**,137–151.
23. X. Querol, A. Alastuey, C.R. Ruiz, B. Artinano, H.C. Hansson, R.M. Harrison, E. Buringh, H.M. ten Brink, M. Lutz, P. Bruckmann, P. Straehl, J. Schneider, *Atmos. Environ.*, 2004, **38**, 6547–6555.
24. J.R. Stedman, *Atmos. Environ.,* 2002, **36**, 4089–4101.
25. C. Hueglin, R. Gehrig, U. Baltensperger, M. Gysel, C. Monn, H. Vonmont, *Atmos. Environ.*, 2005, **39**, 637–651.
26. M. Varea, N. Galindo, J. Gil-Moltó, C. Pastor, J. Crespo, *J. Environ. Monit.,* 2011, **13**, 2471-2476.
27. G. Gilli, D. Traversi, R. Rovere, C. Pignata, T. Schilirò, *Sci. Total Environ.,* 2007, **385**, 97–107.
28. R. Massoud, A.L Shihadeh, M. Roumié, M. Youness, J. Gerard, N. Saliba , R. Zaarour , M. Abboud, W. Farah, N. Aoun Saliba, *Atmos. Res.,* 2011, **101**, 893–901.
29. S. Kong, Y. Ji, B. Lu, Z. Bai, L. Chen, B. Han Z. Li, *J. Environ. Monit.,* DOI: 10.1039/c2em10648e, 2012.
30. Md.F. Khan, K. Hirano, S. Masunaga, *Atmos. Environ.,* 2010, **44**, 2646-2657.
31. S.S. Park, Y.J. Kim, *Chemosphere,* 2005, **59**, 217-226.
32. P. Hegde, A.K. Sudheer, M.M. Sarin and B.R. Manjunatha, *Atmos. Environ.,* 2007, **41**, 7751–7766.
33. A. Marmur, J.A. Mulholland, A.G. Russell, *Atmos. Environ.*, 2007, **41**, 493-505.
34. M. Obadasi, N. Vardar, A. Sofuoglu, Y. Tasdemir, T.M. Holsen, *Sci. Total Environ.*, 1999, **227**, 57-67.
35. M. Rehwagen, A. Müller, L. Massolo, O. Herbarth, A. Ronco, *Sci. Total Environ.,* 2005, **348**, 199–210.
36. M. Varea, N. Galindo, J. Gil-Moltó, C. Pastor, J. Crespo, *J. Environ. Monit.,* 2011, **13**, 2471-2475.
37. H. Guo, S.C. Lee, K.F. Ho, X.M. Wang, S.C. Zou, *Atmos. Environ.*, 2003, **37**, 5307– 5317.
38. O. Amador-Muñoz , R. Villalobos-Pietrini, M.C. Agapito-Nadales ,Z. Munive-Colín , L. Hernández-Mena , M. Sánchez-Sandoval ,S. Gómez-Arroyo , J.L. Bravo-Cabrera , J. Guzmán-Rincón, *Atmos. Environ.,* 2010, **44**, 122–130.
39. A.V. Castellano, J.L. Cancio, P.S. Alemán, J.S. Rodriguez, *Environ. Int.,* 2003, **29**, 475–80.
40. P.C. Vasconcellos, D. Zacarias, M.A.F. Pires, C.S. Pool, L.R.F. Carvalho, *Atmos. Environ.,* 2003,**37**, 3009–3018.
41. K. Karar and A.K. Gupta, *Atmos. Res.,* 2007, **84**, 30–41.
42. M.A. Bari, G. Baumbach, B. Kuch and G. Scheffknecht, *Atmos. Environ.*, 2009, **43**, 4722-4732.
43. W-J. Lee, Y-F. Wang, T-C. Lin, Y-Y. Chen, W-C. Lin, C-C., Ku and J-T. Cheng, *Sci. Total Environ.*, 1995, **159**, 185-200.
44. I.G. Kavouras, P. Koutrakis, M. Tsapakis, E. Lagoudaki, E.G. Stephanou, D. Von Baer. and P. Oyola, *Environ. Sci. Technol.,* 200*1,* **35**, 2288-2294.
45. C. Venkataraman, J.M. Lyons and S.K. Friedlander, *Environ. Sci. Technol.*, 1994, **28**, 555-562.
46. C. Li and R.M. Kamens, *Atmos. Environ.* A, 1993, **27(4)**, 523-532.
47. J.M. López, M.S. Callén, T. García, R. Murillo, M.V. Navarro and A.M. Mastral, *Sci. Total Environ..,* 200*3,* **307**, 111-124.

48. P. Hegde, A.K. Sudheer, M.M. Sarin and B.R. Manjunatha, *Atmos. Environ.,* 2007, **41**, 7751–7766.

Table 1. Some general properties and conditions for the PAH quantification by GC-MS-MS.

		Vapor pressure (mm Hg)[17]	Benzene and total rings	Precursor ion	Quantification ion	CID excitation amplitude[a] (V)	Excitation RF storage level[b] (m/z)	Emission current (μA)	Ion preparation
Phenanthrene	Phe	$6.8x10^{-4}$ 25ºC	3	178	152	1.20	75	80	MRM
Anthracene	An	$1.7x10^{-5}$ at 25ºC	3	178	152	1.20	75	80	MRM
2-/4- Methylphenanthrene	2,4 MePhe	-	3	191	189	0.60	75	80	MS-MS
9-Methylphenanthrene	9MePhe	-	3	191	189	0.60	75	80	MS-MS
1-Methylphenanthrene	1MePhe	-	3	191	189	0.60	75	80	MS-MS
2,5/2,7/4,5 Dimethylphenanthrene	DiMePhe	-	3	206	191	0.90	75	80	MS-MS
Fluoranthene	Flt	$5.0x10^{-6}$ at 25ºC	3 (4)	202	200	1.80	75	80	MS-MS
Pyrene	Py	$2.5x10^{-6}$ at 25ºC	4	202	200	1.80	75	80	MS-MS
Benzo[a]anthracene	BaA	$2.2x10^{-8}$ at 20ºC	4	228	226	2.00	85	80	MRM
Chrysene	Cry	$6.3x10^{-7}$ at 25ºC	4	228	226	2.00	85	80	MRM
Benzo[b]fluoranthene	BbF	$5.0x10^{-7}$ at 20-25ºC	4 (5)	252	250	2.00	90	80	MS-MS
Benzo[j]fluoranthene	BjF	$1.50x10^{-8}$ at 25ºC	4 (5)	252	250	2.00	90	80	MS-MS
Benzo[k]fluoranthene	BkF	$9.59x10^{-11}$	4 (5)	252	250	2.00	90	80	MS-MS
Benzo[e]pyrene	BeP	$5.5x\ 10^{-9}$	5	252	250	2.20	90	90	MRM
Benzo[a]pyrene	BaP	$5.6x10^{-9}$	5	252	250	2.20	90	90	MRM
Indeno[1,2,3-cd]pyrene	IcdP	$\sim10^{-11}$-10^{-6} at 20ºC	5 (6)	276	274	2.70	90	90	MRM
Dibenz[a.h]anthracene	DahA	$1x10^{-10}$ at 20ºC	5	278	276	2.70	90	90	MRM
Benzo[g,h,i]perylene	BghiP	$1.03x10^{-10}$ at 25ºC	6	276	274	2.70	90	90	MRM
Coronene	Cor	$1.5x\ 10^{-11}$	7	300	298	2.70	90	90	MS-MS

[a] Amplitude of waveform applied during CID of precursor ion.
[b] RF voltage in m/z units used during excitation of precursor ion.
MRM= multiple reaction monitoring mode
- = Not available

Table 2. Average concentration of PM10 (μg m^{-3}), ions (μg m^{-3}) and particle-bound PAH (ng m^{-3}) with the corresponding standard deviations for the different periods of sampling carried out in Zaragoza (N= number of samples).

	2001-2002	2003-2004	2008-2009	TOTAL
PM10	40.6±14.7	32.2±12.7	25.6±16.0	32.9±15.2
Cl^-	0.87±0.98	0.69±0.67	0.65±0.69	0.73±0.77
NO_3^-	2.99±2.84	2.68±1.72	3.03±3.90	2.86±2.75
$nmSO_4^{2-}$	4.73±2.63	3.92±2.13	1.79±1.91	3.58±2.49
Na^+	0.69±0.32	0.62±0.33	0.68±0.58	0.65±0.41
K^+	0.41±0.17	0.24±0.09	0.24±0.32	0.29±0.21
Ca^{2+}	1.43±0.64	1.23±0.69	0.83±0.34	1.18±0.63
Phe	0.11±0.10	0.13±0.20	0.17±0.14	0.14±0.16
An	0.03±0.06	0.01±0.02	0.03±0.03	0.02±0.04
2,4 MePhe	0.09±0.09	0.01±0.02	0.05±0.04	0.04±0.06
9 MePhe	0.03±0.03	0.05±0.05	0.05±0.04	0.04±0.04
1 MePhe	0.04±0.04	0.02±0.03	0.06±0.05	0.04±0.04
DiMephe	0.09±0.09	0.06±0.07	0.11±0.10	0.08±0.04
Flt	0.40±0.42	0.23±0.22	0.33±0.38	0.30±0.34
Py	0.40±0.40	0.30±0.26	0.40±0.43	0.36±0.35
BaA	0.49±0.54	0.26±0.42	0.42±0.66	0.37±0.53
Chry	0.70±0.82	0.28±0.32	0.53±0.61	0.47±0.60
BbjkF	0.88±1.15	0.58±0.60	0.95±1.28	0.76±0.99
BeP	0.46±0.55	0.27±0.23	0.31±0.42	0.33±0.40
BaP	0.45±0.48	0.29±0.34	0.28±0.39	0.33±0.40
IcdP+DahA	0.94±0.95	1.08±1.28	0.92±1.10	1.00±1.14
BghiP	0.96±0.89	1.02±1.01	0.42±0.36	0.84±0.88
Cor	1.05±1.06	1.47±1.61	0.30±0.28	1.03±1.31
Total PAH	7.14±6.49	6.05±5.93	5.35±5.96	6.17±6.08
N	32	50	30	112

BbjkF= BbF+BjF+BkF

Table 3. PCA applied after Varimax rotation to samples taken in Zaragoza

	Component				
	PC1	PC2	PC3	PC4	PC5
Cl^-					**.801**
NO_3^-					
$nmSO_4^{2-}$				**.894**	
Na^+					**.898**
K^+					
Ca^{2+}				**.875**	
Phe		**.875**			
An		**.930**			
2,4 MePhe		**.875**			
Flt		**.853**			
Py		**.855**			
BaA	**.760**				
Chry	**.830**				
BbjkF	**.947**				
BeP	**.910**				
BaP	**.881**				
IcdP+DahA			**.729**		
BghiP			**.830**		
Cor			**.864**		
% Variance explained	42.9	17.6	11.7	7.5	5.4

Table 4. Percentage of species apportioned to each source obtained by the PCA-APCS receptor model.

	Industrial+traffic	Coal combustion	Heavy-duty vehicles	Soil resuspension	Marine component
Cl^-	13	4	7	0	76
NO_3^-	21	0	5	59	15
$nmSO_4^{2-}$	0	4	0	96	0
Na^+	2	1	0	11	85
K^+	18	0	1	61	21
Ca^{2+}	0	4	5	91	0
Phe	28	31	21	11	9
An	69	1	30	0	0
2, 4 MePhe	39	0	31	7	23
Flt	54	9	25	3	9
Py	36	12	19	0	33
BaA	39	10	16	0	35
Chry	57	1	16	0	26
BbjkF	71	9	7	4	9
BeP	60	7	18	15	0
BaP	49	14	19	5	14
IcdP+DahA	24	14	36	8	17
BghiP	20	21	43	9	7
Cor	12	24	48	15	0

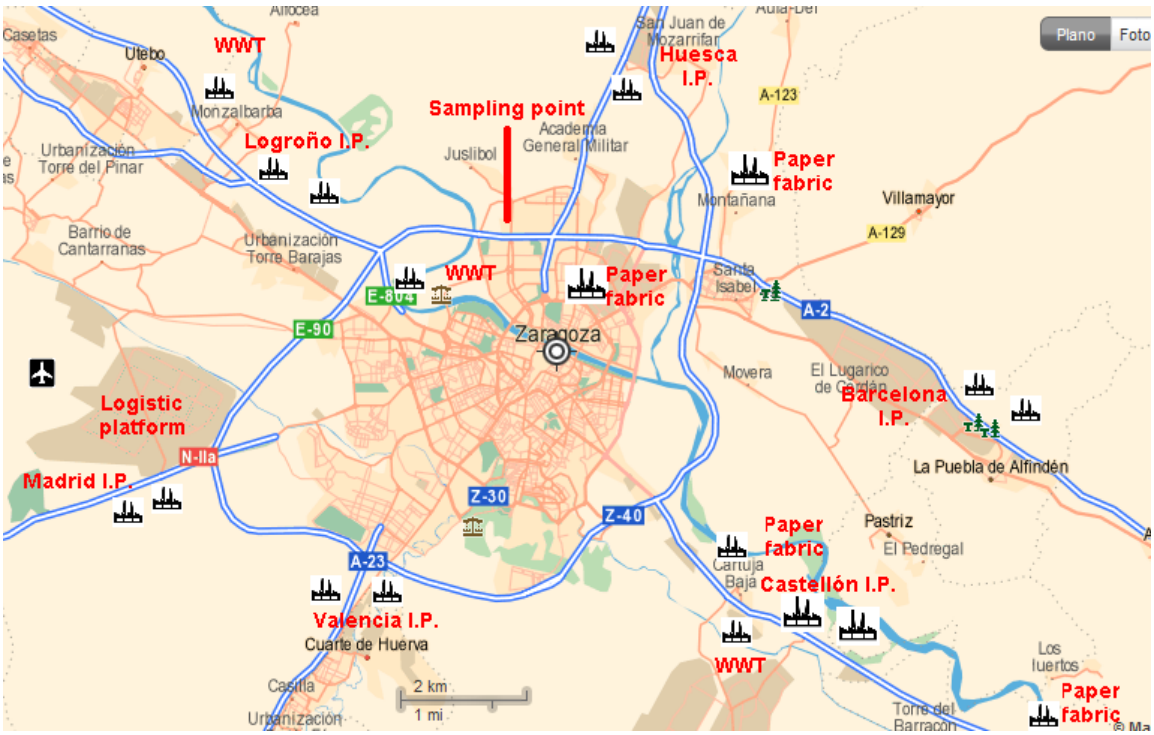

Figure 1. Location of the sampling point at Zaragoza indicating the main roads, industrial parks (I.P.), waste water treatment plants (WWT) and paper fabrics located at the surroundings.

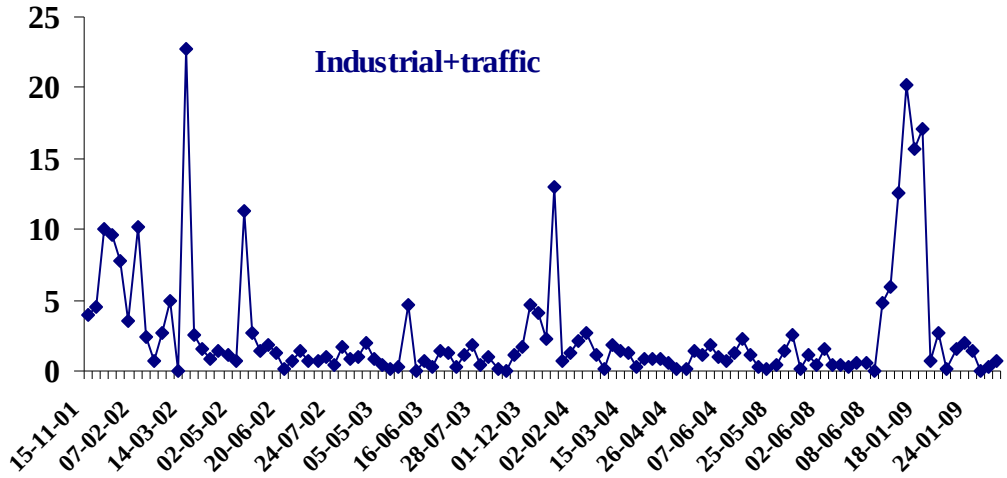
Industrial+traffic
25
20
15
10
5
0
15-11-01
07-02-02
14-03-02
02-05-02
20-06-02
24-07-02
05-05-03
16-06-03
28-07-03
01-12-03
02-02-04
15-03-04
26-04-04
07-06-04
25-05-08
02-06-08
08-06-08
18-01-09
24-01-09

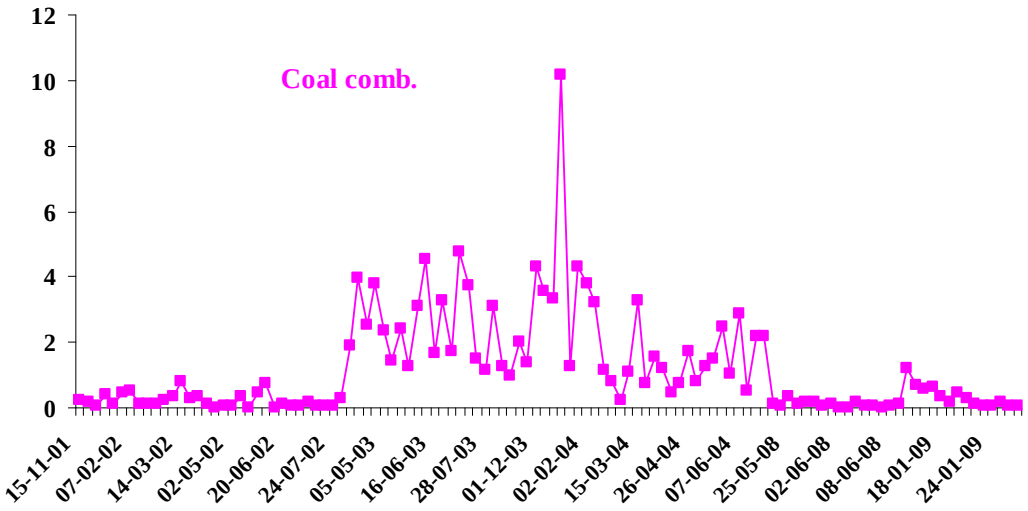
Coal comb.
12
10
8
6
4
2
0
15-11-01
07-02-02
14-03-02
02-05-02
20-06-02
24-07-02
05-05-03
16-06-03
28-07-03
01-12-03
02-02-04
15-03-04
26-04-04
07-06-04
25-05-08
02-06-08
08-06-08
18-01-09
24-01-09

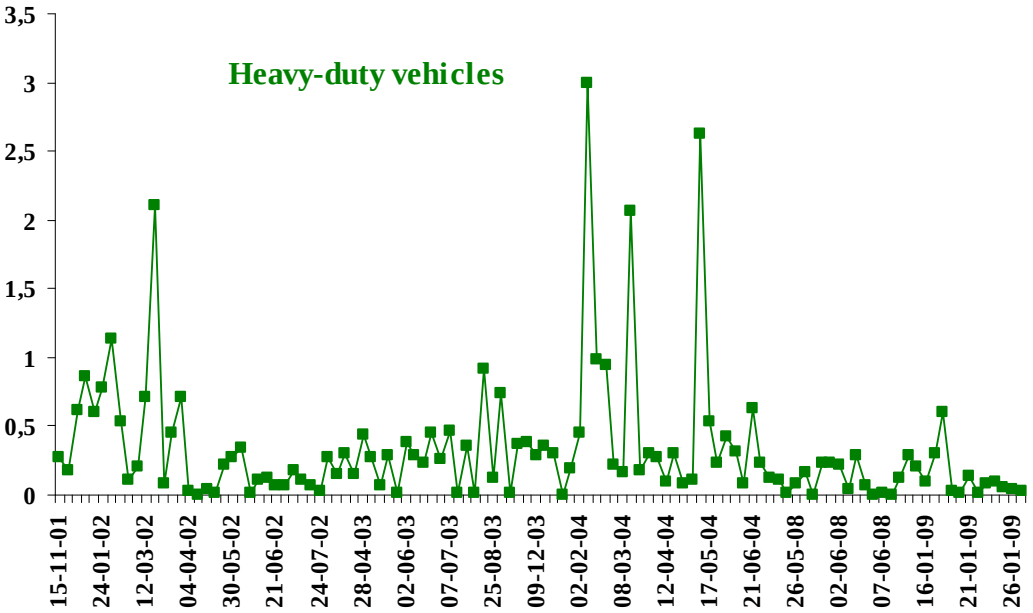
Heavy-duty vehicles
3,5
3
2,5
2
1,5
1
0,5
0
15-11-01
24-01-02
12-03-02
04-04-02
30-05-02
21-06-02
24-07-02
28-04-03
02-06-03
07-07-03
25-08-03
09-12-03
02-02-04
08-03-04
12-04-04
17-05-04
21-06-04
26-05-08
02-06-08
07-06-08
16-01-09
21-01-09
26-01-09

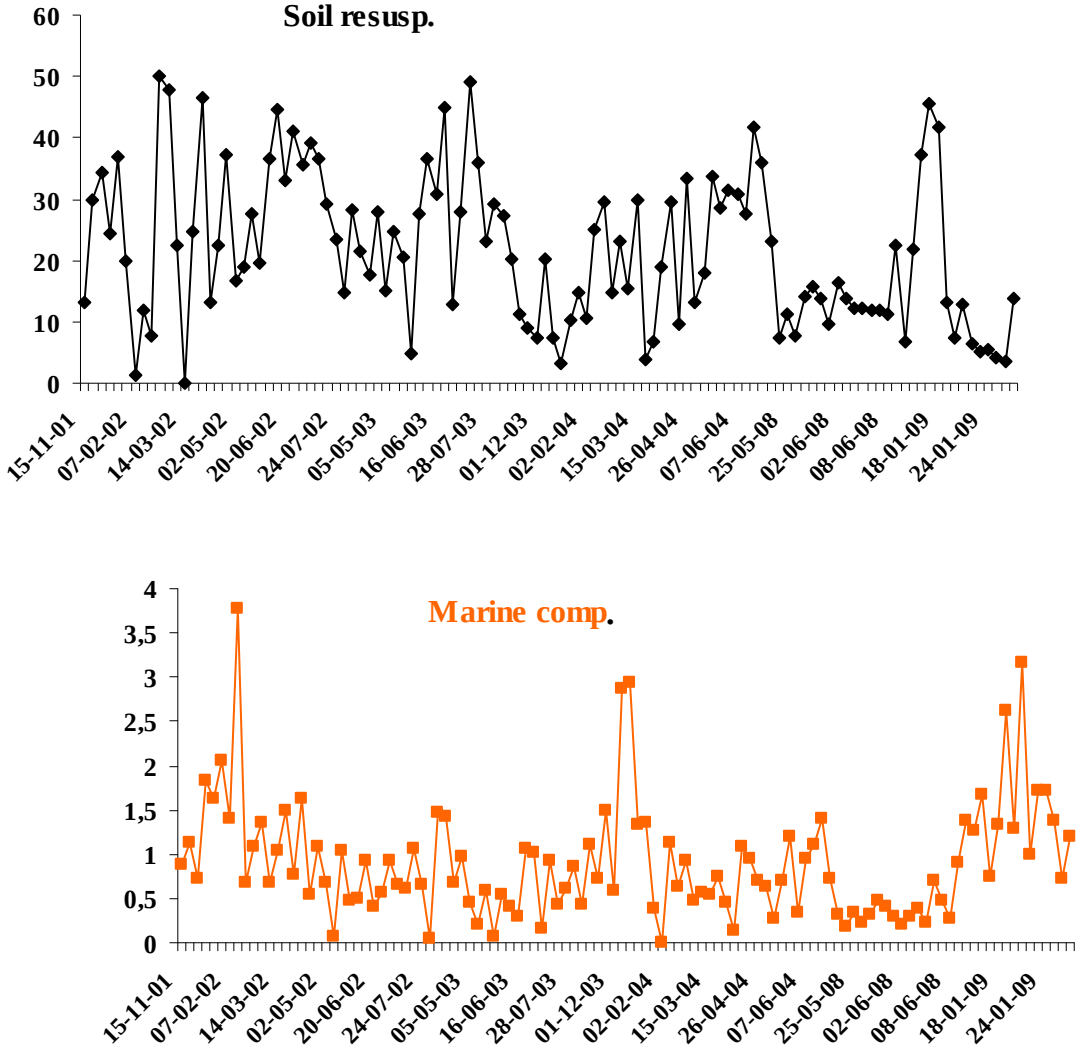

Figure 2. Temporal contribution of each factor (μg m^{-3}) identified by the PCA-APCS receptor model for the Zaragoza samples.

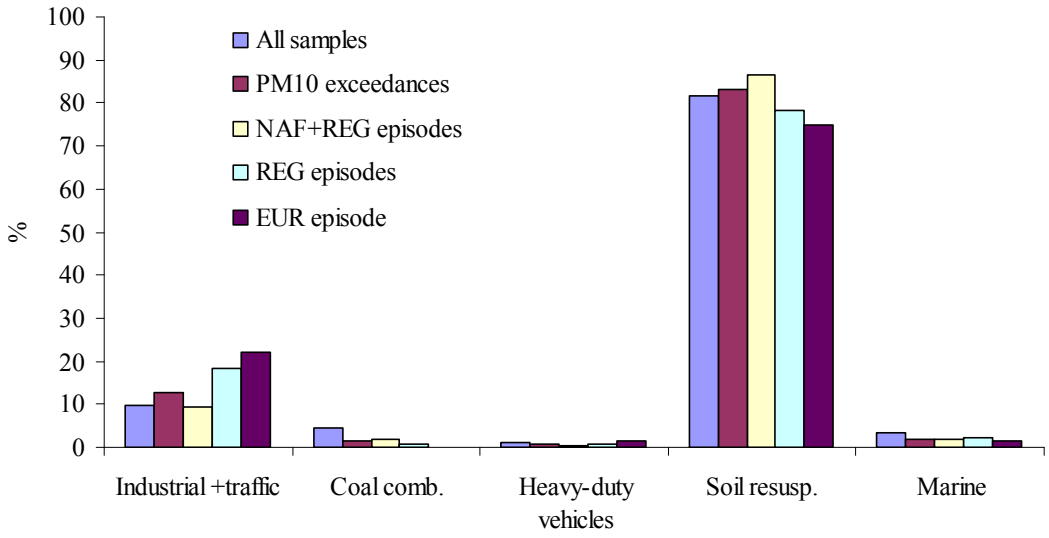

Figure 3. Source contributions (%) obtained by the PCA-APCS receptor model for the average all samples and for the PM10 exceedances according to the scenario type: North-African (NAF+REG) (10/01/02, 12/03/02, 16/05/02, 18/06/02, 19/06/02; 21/06/02, 27/06/02, 22/07/03, 23/06/03, 14/07/03, 17/01/09), regional (REG) (11/03/02, 21/03/02, 16/01/09, 18/01/09) and European scenario (EUR) (13/12/01).

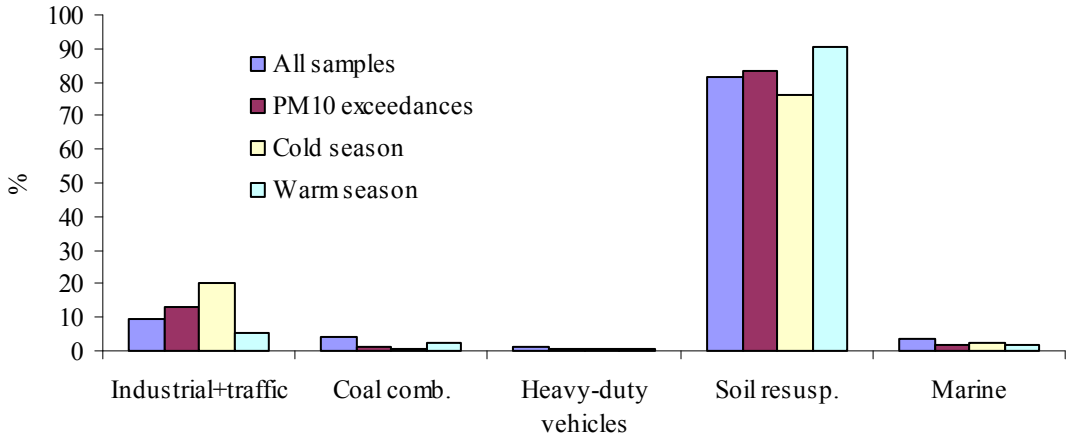

a)

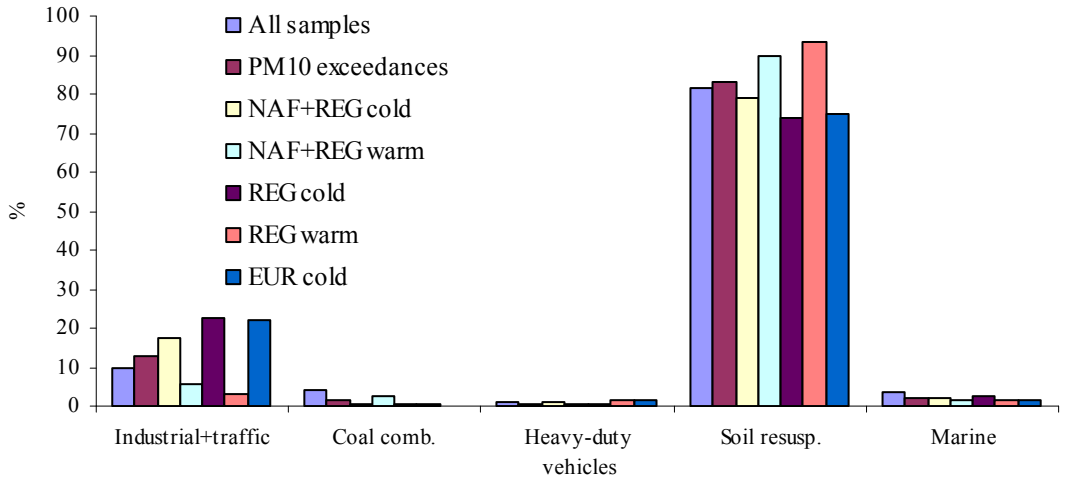

b)

Figure 4. Source contributions (%) obtained by the PCA-APCS receptor model for the average all samples and for the PM10 exceedances as a function of a) the season and b) the backward air trajectories.

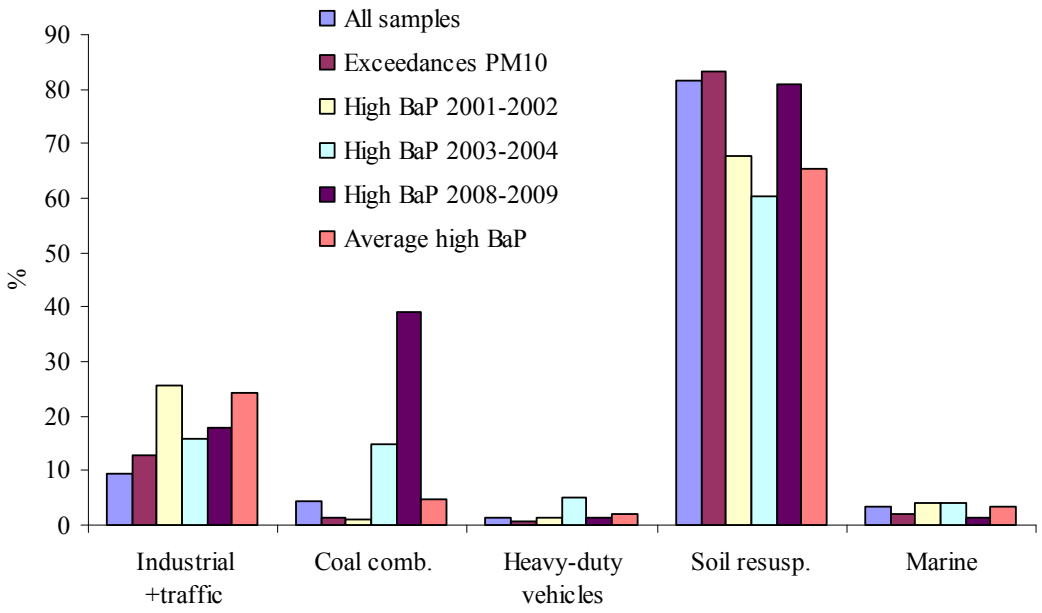

Figure 5. Source contributions (%) obtained by the PCA-APCS for the samples with BaP concentrations higher than 0.6 ng m^{-3} (the upper assessment threshold of BaP according to Directive 2004/107/EC) (these samples have also been classified according to the year of sampling; BaP exceedances: 15/11/2001, 29/11/2001, 13/12/2001, 27/12/2001, 10/01/2002, 24/01/2002, 7/02/02, 14/03/02, 01/12/03, 09/12/2003, 12/01/04, 09/02/04, 15/03/2004, 10/05/2004, 15/01/09, 16/01/09, 17/01/2009 and 18/01/09), for the PM10 exceedances and for the average PM10 samples.

SUPPLEMENTARY INFORMATION

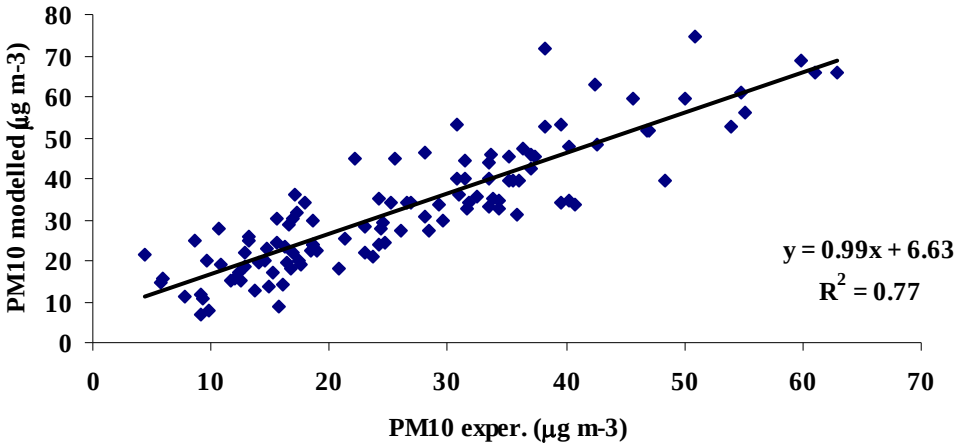

Figure S1. Plot between the experimental and the modelled PM10 obtained by the PCA-APCS receptor model (R^2= correlation coefficient).

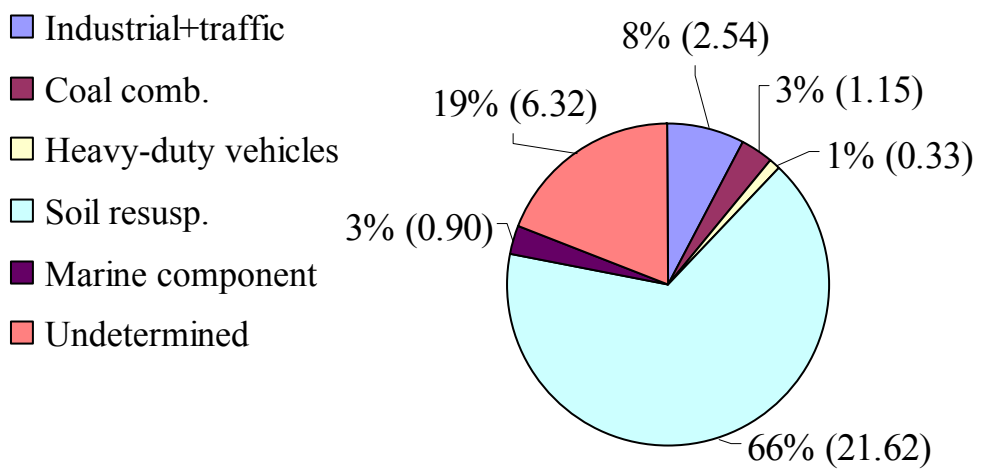

Figure S2. Source contribution (% and μg m^{-3}) for the average PM10 samples obtained by the PCA-APCS receptor model.